

Dima decoction inhibits ulcerative colitis by activating autophagy through modulation of HIF-1 α /BNIP3/Beclin-1 signaling pathway

Yifang Li¹, Rui Wang^{2*}, Zichao Hu² and Jingxia Zhang¹

¹Department of Chinese Medicine Nursing, School of Nursing, Anhui University of Chinese Medicine, Hefei, Anhui, China

²Department of Gastroenterology, The First Affiliated Hospital of Anhui University of Chinese Medicine, Hefei, Anhui, China

Abstract: During the active phase of ulcerative colitis(UC), mitochondrial autophagy is an important antagonistic mechanism. Our investigation examines the regulatory effect of Dima decoction on UC inflammation via the autophagy pathway. SD rats were divided into 5 groups ($n = 10$): normal control (NC) model, mesalazine, Dima decoction treatment and Dima decoction combined with YC-1 (inhibitor) group. Results showed that treatment of Dima decoction effectively ameliorated the symptoms of UC. Drug-containing serum from Dima decoction treated rats leads to an significantly increase in IL-4 and IL-10 content in HT-29 cells, while also causing a decrease in IL-1 β and IL-6 content. Moreover, protein level and mRNA level of HIF-1 α , BNIP3, Beclin-1 were obviously up-regulated. In addition, protein level of LC3B II and the ratio of LC3B II/I were dramatically promoted after Dima decoction serum administration. The protein level of Bax was notably decreased in TH-29 cells after Dima decoction serum supplement, while that of Bcl-xl was remarkably up-regulated. In conclusion, Dima decoction significantly alleviated the symptoms of UC. The regulation could involve modulation of the hypoxia-inducible HIF-1 α /BNIP3/Buclin-1 pathways, leading to effects on mitochondrial autophagy and inflammation. These findings offer new insights into the mechanism of Dima decoction for treating UC.

Keywords: ulcerative colitis; Dima decoction; HIF-1 α /BNIP3/Beclin-1 signal pathway; mitophagy;

Submitted on 19-07-2023 – Revised on 15-04-2024 – Accepted on 19-09-2024

INTRODUCTION

Currently believed that ulcerative colitis (UC) clinically characterized by bloody stools or diarrhea, accompanied by mucosal damage, ulcers, colon shrinkage, and other intestinal manifestations. It is currently considered an autoimmune intestinal disease. (Cui *et al.*, 2021). UC patients present a state of recurrent flare-ups or prolonged persistence of the above symptoms (Zhong *et al.*, 2022). Current statistics show that the prevalence of UC in developed countries is 200-500 per 100,000 people, and a similar trend is observed globally (Agrawal *et al.*, 2022). The development of UC is intricate due to the interplay of various factors, including but not limited to immune responses, gut microbiota, emotional stress, oxidative damage and other elements (Niu *et al.*, 2021). And currently, UC treatment drugs have problems such as unsatisfactory therapeutic effects, high prices, and high incidence of adverse reactions (Niu *et al.*, 2021). Developing safe and effective alternative therapies for prevention and management of UC can help address the aforementioned issues.

Autophagy in mammals stands as a pivotal and foundational cellular mechanism, enabling cells to adapt to their surroundings and uphold internal stability. In the past decade, numerous studies have identified multiple genes related to autophagy linked with UC and defects in this process increase susceptibility to colitis in mice

*Corresponding author: e-mail: dsf221@163.com

(Zhou *et al.*, 2020). Some medications for treating UC also work through mechanisms that control the disease by regulating autophagy (Larabi A *et al.*, 2020). Additionally, mice lacking autophagy genes exhibited heightened release of pro-inflammatory cytokines (du Plessis *et al.*, 2021), which are particularly crucial for the treatment and prognosis of UC patients.

Modern research indicates that oxidative stress is a crucial factor in triggering intestinal inflammation in UC (Zhang SM *et al.*, 2023). When excessive reactive oxygenspecies (ROS) exceeds the antioxidant capacity of cells, it triggers oxidative stress, and mitophagy can counteract oxidative stress. Mitophagy is a selective autophagy, proposed by Lemasters (Lemasters JJ, 2005). Mitophagy can counteract damage caused by oxidative stress and protect cells. The mitophagy of colonic mucosal epithelial cells as a protective mechanism against UC intestinal inflammatory response has been studied and confirmed, among which HIF-1 α / The BNIP3/Beclin-1 pathway is closely related to mitophagy(Chen, Y *et al.*, 2023).

In modern clinical research, in UC treatment, the methods of removing dampness, promoting blood circulation and detoxifying are extensively employed. Dima decoction is an empirical prescription from the Anhui Hospital of Chinese Medicine for treating UC, which includes purslane (*Portulaca oleracea* L.), *astragalus* and *Euphorbia humifusa* as the main ingredients. The main function of Dima decoction is replenishing “qi” to invigorate the spleen and activating blood circulation and

detoxicating. Certain studies have indicated that purslane mitigates lung inflammation and alleviates liver cell inflammation induced by ethanol, as well as joint inflammation triggered by zymosan, through the reduction of pro-inflammatory factors. (Zhang *et al.*, 2022). The bioactive substances in astragalus membranaceus can promote autophagy, which has been confirmed in research related to the treatment of Parkinson's disease (Tan *et al.*, 2020). Furthermore, the enhanced autophagy induced by astragalus flavonoids also inhibited pulmonary fibrosis in the model mice (Xu *et al.*, 2018). Paratocarpin E found in *Euphorbia humifusa* Wild also enhances autophagy and induced apoptosis in human breast carcinoma cells. (Gao *et al.*, 2016). Above findings demonstrated the potential of Dima decoction for treating UC, which may be related to its regulation of autophagy. This research primarily investigated the impact of Dima decoction on intestinal epithelial inflammation and mitophagy in UC rats, as well as the underlying mechanisms using the HT-29 inflammatory cell model.

MATERIALS AND METHODS

Reagents

McCoy's 5A medium: Procell Life Science & Technology Co., Ltd. (Wuhan, China); PBS: Doublehelix Biology S&T Co., Ltd. (China); pancreatin: Beyotime (China); TNF- α : Sino Biological Inc. (Beijing, China); fetal bovine serum: Sijiqing (Hangzhou, China); LPS: Sigma (USA); and YC-1: Medchem Express (USA). TRIpure, Super M-MLV reverse transcriptase, RNase inhibitor, 2 \times Power Taq polymerase chain reaction (PCR) MasterMix, and SYBR Green: BioTeke Corporation (Beijing, China). Total protein extraction kit, BCA protein determination kit, primary and secondary antibody removal solutions, sodium dodecyl sulfate-polyacrylamide gel electrophoresis (SDS-PAGE) rapid gel preparation kit, Western washing buffer, SDS-PAGE electrophoresis solution (dry powder), SDS-PAGE protein loading buffer, and ECL luminescent solution: Wanlei Biotechnology Co., Ltd. (Beijing, China). HIF-1 α , BNIP3, Beclin-1, LC3B II/I, Bax, Bcl-xl, goat anti-rabbit IgG-HRP and reference antibody β -actin were purchased from Wanlei Biotechnology Co., Ltd. Pre-stained protein molecular weight standard was purchased from Fermentas (Canada). The PVDF membrane: Millipore (China) Co., Ltd. (Shanghai, China). Interleukin 6 (IL-6) enzyme-linked immunosorbent assay (ELISA) kit, IL-1 β ELISA kit, IL-4 ELISA kit, IL-10 ELISA kit and BCA protein quantification kit were purchased from Wanlei Biotechnology Co., Ltd. HIF-1 α inhibitor YC-1: Selleck (USA). Mesalazine granules (500 mg/bag, lot number: 191002, drug standard number: H20040727): Ethypharm (France).

Animals and cells

SPF SD rats were obtained from Byrness Weil Biotech Co., Ltd. in Chongqing, China, under the license number SCXX (Chongqing) 2017-0003. For the animal experiments, an equal number of male and 6 to 8-week-old female mice, weighing 250 \pm 12g, were used. All animal handling protocols adhered to both the Guidelines for Care and Use of Laboratory Animals (NIH publication no. 85-23, revised 1985) and the Animal Management Regulations set forth by the Ministry of Health of the People's Republic of China (document no. 55, 2001). The experiments received approval from the Animal Ethics Committee of Anhui University of Chinese Medicine, Anhui, China, under the ethical number AHUCM-mouse-2022084. The animals were fed adaptively for 1 week before use. The HT-29 (in situ colon cancer cell) cell line grew adherently in a single layer, with a colony formation rate of 40%. The tumorigenicity of nude mice was 100%.

Dima decoction preparation

The Dima decoction comprised purslane 30g, raw astragalus 30g, coptis 6g, cortex phellodendri 10g, betel nut 10g, *Euphorbia humifusa* 30g, fried atracylodes 10 g, costusroot 10g and 10g red peony root. All medicinal materials have been identified by Gao Jiarong, the Chief Pharmacist from the same institution as the corresponding author. All medicine materials were soaked in distilled water at 25 $^{\circ}$ C for 60 min, keeping the water about 2 cm above the medicine materials when they were gently pressed. The medicinal ingredients were subjected to boiling for 30 minutes at high temperature, followed by simmering for an additional hour. Subsequently, 300 mL of the resulting medicinal solution was collected for subsequent utilization, stored in the refrigerator at 4 $^{\circ}$ C. Its concentration was 0.49g/mL.

Modeling, grouping and intervention methods

2,4,6-trinitrobenzene sulfonic acid and a high-fat feeding regimen with ethanol was employed for inducing an active UC phenotype in rats (Vardareli *et al.*, 2003). Then the rats, totaling 50 in number, were allocated randomly to one of five groups (n=10). There were: normal control (NC), model, mesalazine, Dima decoction treatment, and Dima decoction combined with YC-1 (inhibitor) groups. Apart from the NC group, rats in the remaining groups were administered honey water ad libitum daily, along with gavage of heat-melted lard (15g/kg) and spirit (40% vol) 20 mL/kg every other day over the course of 20 d. Meanwhile, the rats were injected with antigen emulsion on 6 and 20 d. Subsequently, all rats underwent anesthesia with a dose of 2mL/kg of 2% sodium pentobarbital following a 36-hour fasting period, followed by enema treatment. The NC group rats received a 2.5 mL enema of normal saline, while the remaining rats were administered a 2.5mL enema containing a mixture of 5% TNBS and 50% ethanol in a ratio of 12:5. Rats with diarrhea, pus and blood stools, positive occult blood test in stool routine, reduced water and diet, decreased activity, low and yellow

urine, sticky and unformed stools and yellow tongue coating were considered successful in modeling. For 14 days, administer normal saline to NC and model group rats via gavage (1mL/100 g/d). Those in Dima decoction treatment group received Dima decoction at a dose of 17.0g/kg by gavage (1mL/100 g/d). Administer mesalazine granules 3.0g/kg/d to mesalazine group rats by gavage for 14 d. For rats in inhibitor group, they were treated not only with Dima decoction at a dose of 17.0g/kg by gavage (1mL/100 g/d), but also with YC-1 intravenously 30 min after gavage at a dosage of 2mg/kg/d for same period.

Preparation of drug-containing serum

From each group, three rats were chosen at random to obtain drug-containing serum. Blood samples were taken from the abdominal aorta under sterile conditions, two hours after the final administration. The serum was then separated via centrifugation (2000 rpm, 15 min). Following this, inactivate the serum according to the operational temperature (56°C) and duration (30min) documented in the literature to eliminate bacteria (Watanabe, *et al.*, 2020)

Grouping and administration of HT-29 inflammatory cells

HT-29 cells were cultured in McCoy's 5A medium supplemented with 10% fetal bovine serum and 0.1% double antibody (100 U/mL penicillin and 100 mg/L streptomycin). The cells were maintained in a 37°C humidified incubator with 95% O₂ and 5% CO₂ (Chen, *et al.*, 2022). When growing to a density of about 90%, the cells were subcultured in a ratio of 1:2. When cells adhered to the wall reached 70%, the experimental cells were divided 7 groups, including normal control (NC), model, mesalazine, low dose Dima decoction (LD), medium dose Dima decoction (MD), high dose Dima decoction (HD), and high dose Dima decoction combined with YC-1 (inhibitor) group according to random number method. Cells in the NC group were cultured using a complete medium. In contrast, the cells in the other groups were exposed to TNF- α (20 μ g/L) for 12 hours. Subsequently, LPS (1 mg/L) was administered for an additional 12 hours to induce the HT-29 inflammatory cell model. 10% serum from rats in model group and 10 % drug-containing serum from mesalazine group were added to model and mesalazine group, respectively. The cells in Dima decoction treatment groups received drug-containing serum from Dima decoction treated rats as mentioned before at a dose of 5%, 10% and 20% as low, medium and high dose, respectively. For inhibitor group, the cells received 10 % drug-containing serum from Dima decoction treated rats and 5 μ M YC-1 1 h after serum treatment. After 24 h of incubation, cells and supernatants from each group were collected by centrifugation (1000 g, 10 minutes) for subsequent use.

Intestinal histopathological analyses

Wash the tissue taken from the lesion of the sigmoid colon of the euthanized rats with PBS. After washing, fixed the tissue with 4% paraformaldehyde for 72 hours. Then the tissues were dehydrated, embedded in paraffin, and then sectioned into slices of 4 μ m thickness. The sections were sequentially stained with hematoxylin dye and eosin dye for 10 min and 30 s, respectively. The optical microscope (400 \times magnification) was used to observe the pathological changes in the rat colon tissue.

Observation of mitophagy by transmission electron microscopy (TEM)

The collected colon tissue samples were processed by fixation, dehydration, and embedding, followed by sectioning into 1- μ m-thick slices. The tissue sections underwent staining with a methylene blue dye solution at 60°C for 30 seconds, then stained with composite dye for 10 s, and cut to obtain 50-nm ultra-thin sections. After that, these sections were stained with uranyl acetate and lead staining solution for 10 and 12 min at ambient temperature, respectively. Prepared slices were examined using a transmission electron microscope (HITACHI Corporation, Hitachi, Japan, 3000 \times magnification).

Detection of inflammatory factors in the supernatant of HT-29 cells by ELISA

The supernatant was separated by centrifugation, as described above. The level of interleukin 1 β (IL-1 β), interleukin 6 (IL-6), interleukin 10 (IL-10) and interleukin 4 (IL-4) were measured by ELISA according to the manufacturer's instructions. A microplate reader was used to record the absorbance (OD value) at a wavelength of 450 nm, and the concentration of cytokines in a sample was determined according to the standard curve.

Western blot (WB) analysis

WB was used to detect the expression levels of LC3B II/I, HIF-1 α , BNIP3, Beclin-1, Bax, and BCL-x1 proteins in HT-29 cells. The collected cells underwent two washes with ice-cold PBS solution, lysed using a buffer containing protease inhibitors. The BCA protein concentration determination kit was used for protein quantification. Protein (15 μ g) was taken to electrophoresis on polyacrylamide gel, and subsequently transferred onto a PVDF membrane. The membrane was incubated with 2% bovine serum albumin for 2 h at room temperature, followed by overnight incubation with the primary antibody at 4°C. Following this, an HRP-labeled secondary antibody (goat anti-mouse or rabbit IgG) was applied and incubated for 2 hours at room temperature. The membranes underwent a final washing step of 3 times with TBST for 5 min each. Chemiluminescent substrate was added to expose using the exposure instrument. Lab Image software (Kapelan GmbH, Leipzig, Germany) was used for grayscale analysis to calculate the relevant protein levels.

Table 1: Primer sequence

Primer	Sequence (5'-3')	Length/bp
HIF- α	Upstream :AGTGTACCCTAACTAGCCG	159
	Downstream :CACAAATCAGCACCAAGC	
BNIP3	Upstream: TTCCAGCCTCGGTTTCTA	168
	Downstream: CAATGCTATGGGTATCTGTTTC	
Beclin-1	Upstream: CGTGGAAATGGAATGAGAT	110
	Downstream: CGTAAGGAACAAGTCGGTAT	
β -actin	Upstream: GGCACCCAGCACAAATGAA	168
	Downstream: TAGAAGCATTTCGGGTGG	

Table 2: Levels of inflammatory factors in different groups

Group	IL-6	IL-1 β	IL-4	IL-10
NC	34.05 \pm 2.29	11.12 \pm 1.52	27.19 \pm 3.04	106.34 \pm 3.21
Model	148.21 \pm 6.01a	85.27 \pm 4.37a	16.04 \pm 1.20c	21.65 \pm 1.98a
Mesalazine	41.67 \pm 2.65d	17.17 \pm 1.03d	40.31 \pm 1.89ce	75.18 \pm 3.35cd
Low dose	92.14 \pm 5.03ae	57.98 \pm 4.96bf	25.05 \pm 2.47	44.63 \pm 4.58ae
Medium dose	70.82 \pm 5.36bd	41.07 \pm 5.02be	26.84 \pm 1.98	71.02 \pm 6.29ce
High dose	47.36 \pm 4.49d	20.88 \pm 3.61d	38.26 \pm 1.20cf	83.46 \pm 8.91cd
Inhibitor	118.92 \pm 8.87af	75.32 \pm 7.50a	13.92 \pm 2.01c	28.39 \pm 5.23a

Significant differences: a: Model vs. NC groups, b: Low dose, Medium dose, Inhibitor vs. Model, c: Mesalazine vs. other groups, d, e, f: High dose vs. other groups.

Table 3: mRNA expression level of the receptor in the HIF-1 α /BNIP3/Beclin-1 signaling pathway

Group	HIF- α	BNIP3	Beclin-1
NC	1.00 \pm 0.05	1.00 \pm 0.09	1.00 \pm 0.03
Model	2.16 \pm 0.18b	1.97 \pm 0.17b	2.05 \pm 0.11b
Mesalazine	4.20 \pm 0.23ae	4.48 \pm 0.41ad	3.89 \pm 0.12ae
Low dose	2.68 \pm 0.02b	2.25 \pm 0.17b	2.65 \pm 0.22a
Medium dose	3.30 \pm 0.33bf	2.99 \pm 0.28af	3.27 \pm 0.30bf
High dose	5.25 \pm 0.34ae	5.60 \pm 0.29ad	4.50 \pm 0.16bf
Inhibitor	0.86 \pm 0.07e	1.95 \pm 0.11b	1.78 \pm 0.29c

Significant differences: b: Model vs. NC, a, e: Mesalazine vs. other groups, f: High dose vs. other groups

Real-time quantitative PCR (RT-qPCR) analysis

mRNA levels of the pathway proteins in HT-29 cells were analyzed employing this technique. HT-29 cells were processed with Trizol reagent to extract total RNA, followed by cDNA synthesis using the Maxime RT Premix kit (Promega, Beijing, China). The purity of RNA was measured using the UV-spectrophotometer at A260/A280. 1 μ g RNA sample was used to synthesis cDNA. Reverse transcription was performed for 10 min at 25°C, followed by 50 min at 42°C and 5 min at 85°C. The amplification was carried out in the following manner: it commenced with an initial denaturation step for 4 min at 94°C, followed by 35 cycles consisting of denaturation for 20 s at 94°C, annealing for 30 s at 60°C, and extension for 30 s at 72°C. The calculation of relative mRNA expression using the 2- $\Delta\Delta$ Ct method utilized β -actin as the internal reference. The primer sequences are detailed (table 1).

STATISTICAL ANALYSIS

It was conducted using SPSS software (version 25.0, IBM Corp., Armonk, NY, USA). Results were presented as mean \pm standard deviation from 3 independent experiments. A t test was used to analyse the significance of differences, with P<0.05 considered indicative of statistical significance.

RESULTS

Pathological morphology of colonic mucosa

Results are shown in fig. 1. Rats of NC group showed normal colonic mucosal tissue, with no lesions of pathological significance (fig. 1A). However, the pathological examination of colonic mucosal tissue in model rats revealed significant destruction of the mucosal structure, extensive inflammatory cell infiltration, loss of intestinal crypt architecture and disruption of the

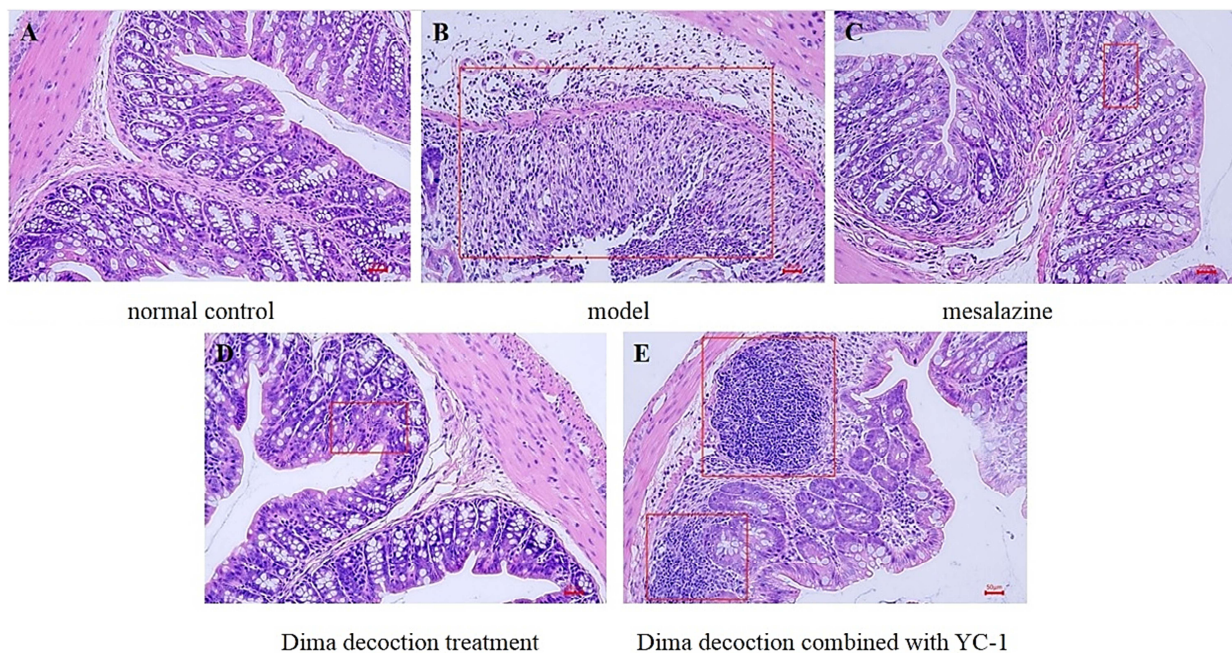


Fig. 1: Effect of Dima decoction on the histopathology of the colon of the UC model rats.

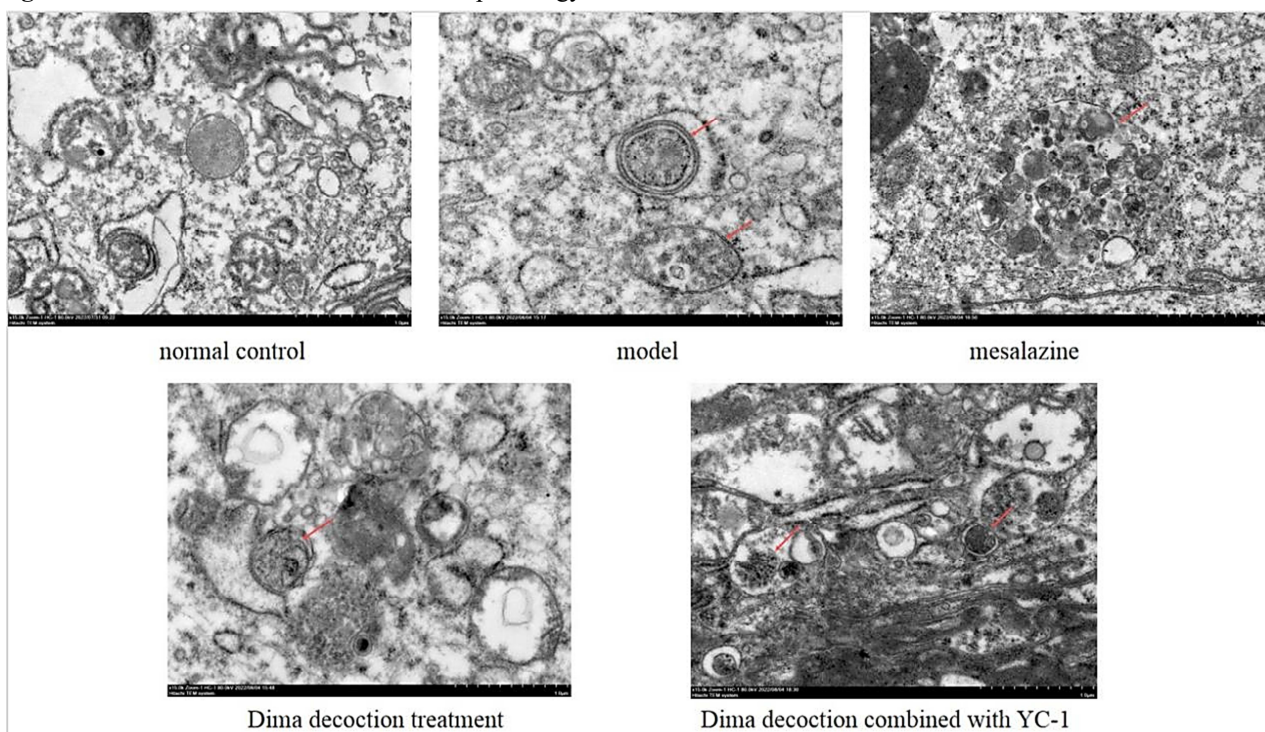


Fig. 2: Effect of Dima decoction on the mitophagy of the colon in UC model rats. (A) normal control (NC) group; (B) model group; (C) mesalazine group; (D) Dima decoction treatment group; (E) Dima decoction combined with YC-1 (inhibitor) group.

epithelial layer, which are characteristic symptoms of UC progression (fig. 1B). From fig. 1C we could see that the microscopic features of UC were significantly improved. The administration of Dima decoction restored the damaged tissue architecture, as indicated by the recovery of crypt structure and a decrease in inflammatory cell infiltration (fig. 1D). Besides, the similar results were

observed with model group, suggesting a strong inhibitory effect of YC-1 on the biological activity of Dima decoction (fig. 1E).

Mitophagy in colonic mucosal tissue

The microstructure changes of colon tissues were observed by TEM. No obvious abnormalities were found

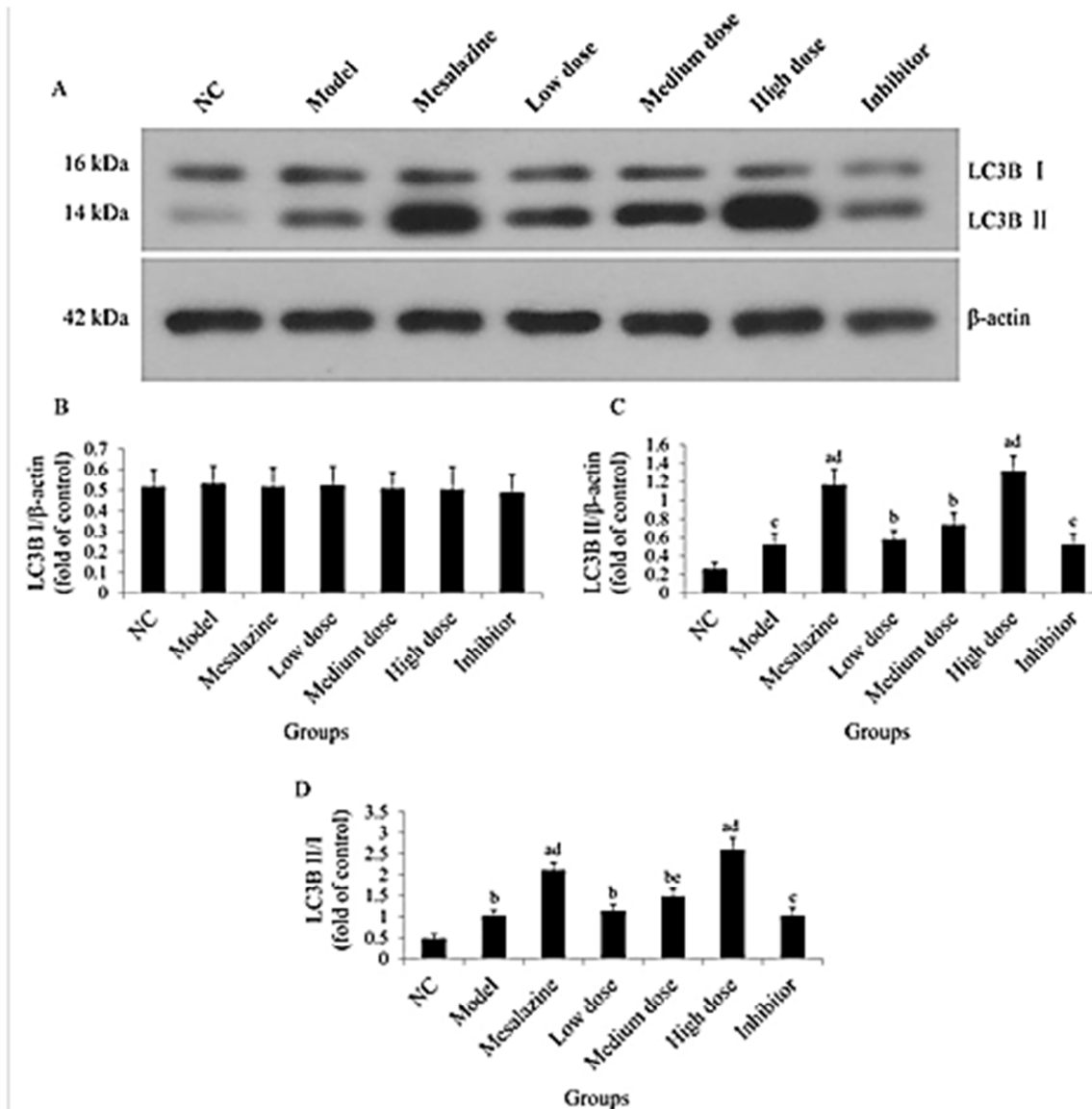


Fig. 3: Effect of autophagy protein expression levels in each group. Compared with black group, ^a $P < 0.001$, ^b $P < 0.01$, ^c $P < 0.05$; compared with model group, ^d $P < 0.01$.

in the lipid inclusions in the mitochondria and the outer chamber of the mitochondria in the NC group (fig. 2A). Furthermore, the microvilli on the epithelial cells were orderly, their tips were apparent, and tight junctions were intact. However, the images from model group showed mitochondrial damage, such as lipid inclusions in the mitochondria and swelling of the outer chamber of the mitochondria, but autophagosomes were invisible (fig. 2B). In addition, the microvilli within the colon were sparse and shortened, the tight junctions were disrupted, with the gaps between cells were enlarged. In stark contrast, supplementation with mesalazine and Dima decoction significantly improved the damaged ultrastructure in UC (fig. 2C, D). Relative to the model group, the Dima decoction groups showed autophagosomes with double lipid membrane structure, as well as mitophagy at endoplasmic reticulum-

mitochondrial contact sites. YC-1 administration obviously weakened the effect of Dima decoction, with lessened autophagosomes, reduced endoplasmic reticulum-mitochondrial contact sites and disrupted ultrastructure (fig. 2E).

Levels of inflammatory factors in the supernatant of HT-29 inflammatory cells

The concentrations of IL-1 β , IL-6, IL-4 and IL-10 proteins in the supernatant of HT-29 inflammatory cells were evaluated using ELISA assay (table 2). Compared with NC group, the expression levels of IL-1 β and IL-6 in model group were significantly up-regulated ($P < 0.001$), while those of IL-4 and IL-10 were significantly down-regulated ($P < 0.001$ or $P < 0.05$). However, it was reversed after Dima decoction serum treatment. In comparison with model group, the levels of IL-6 and IL-1 β were

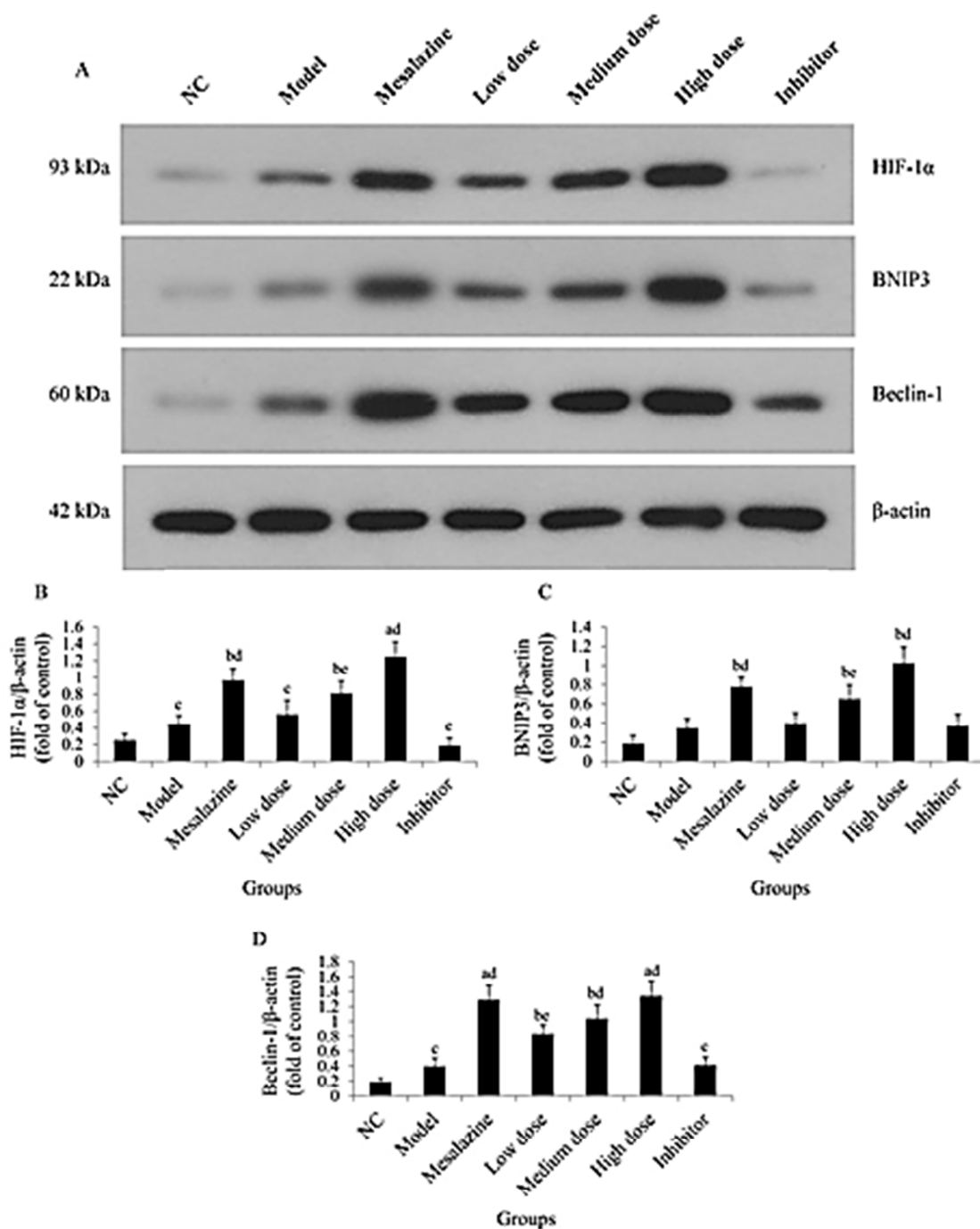


Fig. 4: Effects of the expression levels of autophagy signal pathway proteins in each group. Compared with black group, ^a $P < 0.001$, ^b $P < 0.01$, ^c $P < 0.05$; compared with model group, ^d $P < 0.01$, ^e $P < 0.05$.

significantly decreased ($P < 0.001$, $P < 0.01$ or $P < 0.05$) and the levels of IL-4 and IL-10 were observably increased ($P < 0.001$, $P < 0.01$ or $P < 0.05$), especially after high dose Dima decoction serum administration. In consistent with the results observed in the previous images, YC-1 obviously inhibited the effect of Dima decoction serum.

Expression of autophagy protein in HT-29 cells

Results of protein expression of LC3B I and LC3B II in HT-29 cells were displayed in fig. 3A. The model group

exhibited a marked elevation in both LC3B II levels and the LCII/LCI ratio compared with the NC group ($P < 0.05$ and $P < 0.01$, respectively). The reversal occurred after administration of mesalazine and Dima decoction serum. The administration of mesalazine serum significantly enhanced the level of LC3B II and the LCII/LCI ratio compared with NC group ($P < 0.001$). Notably, high-dose Dima decoction serum exhibits effects comparable to those of Mesalazine, with significant higher expression compared with NC and model group ($P < 0.01$). YC-1

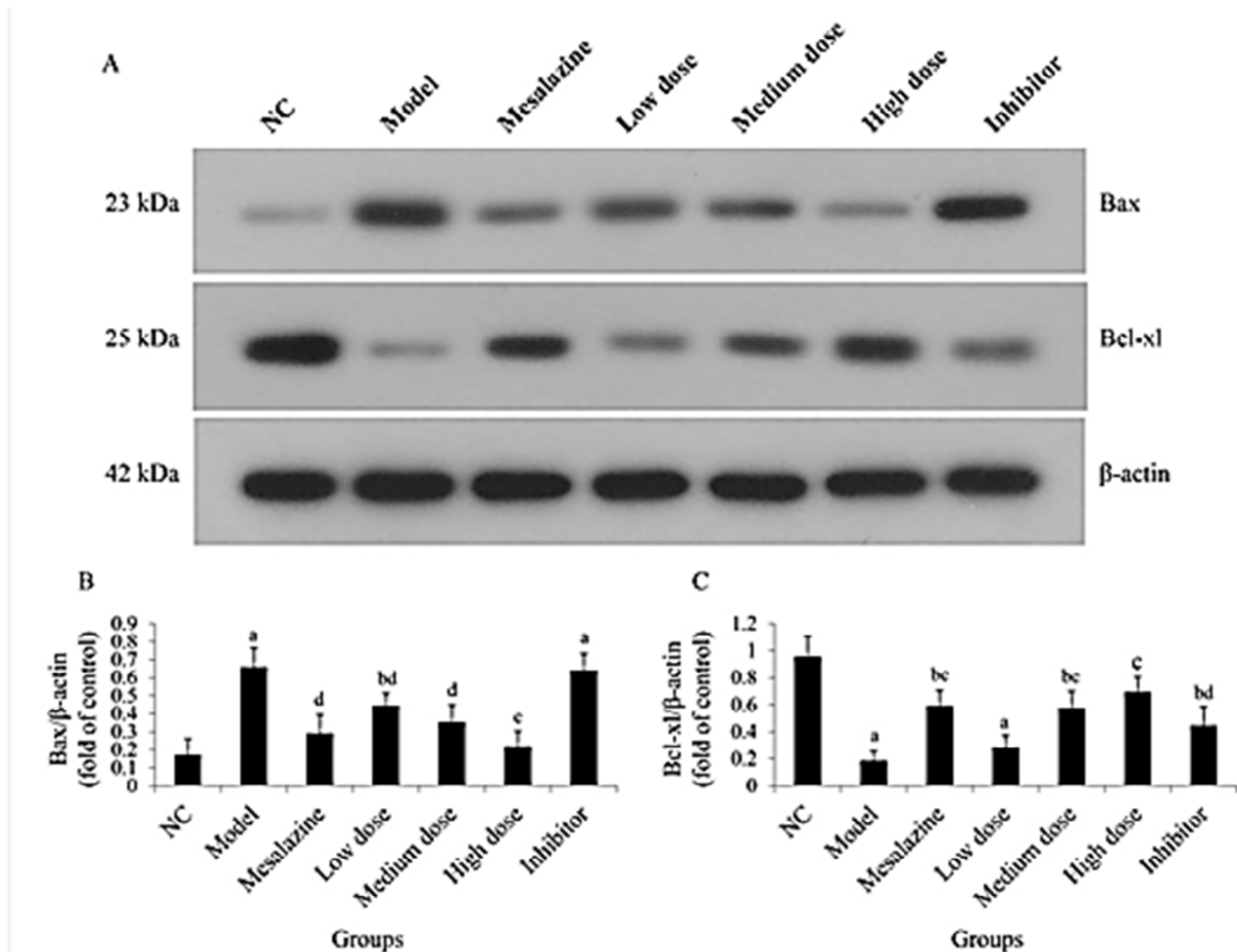


Fig. 5: Effects of the expression levels of apoptosis-related proteins in each group. Compared with black group, ^a $P < 0.01$, ^b $P < 0.05$; compared with model group, ^c $P < 0.01$, ^d $P < 0.05$.

exhibited a profound inhibition of the efficacy of Dima decoction serum, with negligible alterations observed relative to the model group ($P > 0.05$).

The protein expression of the autophagy signaling pathway in HT-29 cells

The protein expression results in HT-29 cells were displayed in fig. 4A. The model group demonstrated differing degrees of increased expression levels of HIF-1 α , BNIP3, and Beclin-1 relative to the NC group ($P < 0.05$ or $P > 0.05$). Subsequent to supplementation with Mesalazine serum, the expression levels of these proteins were markedly higher than those observed in the model group ($P < 0.01$). Remarkably, the administration of Dima decoction serum, particularly at a high dose, markedly enhanced the levels of HIF-1 α , BNIP3, and Beclin-1 in relation to the model group ($P < 0.01$). The inhibiting effect of YC-1 on the protein expression of HIF-1 α , BNIP3 and Beclin-1 after Dima decoction serum treatment was similar to that on autophagy protein.

Apoptosis-related protein expression levels in HT-29 cells

The results of protein levels of Bax and Bcl-xl in HT-29 cells were displayed in fig. 5A. Compared to the NC group, Bax expression markedly increased in the model group ($P < 0.01$), whereas Bcl-xl expression markedly decreased ($P < 0.01$). Mesalazine serum treatment up-regulated the expression level Bax and down-regulated that of Bcl-xl greatly ($P < 0.05$ and $P < 0.01$, respectively). Dima decoction serum, particularly at a high dose, showed similar effects to Mesalazine. Compared with model group, Dima decoction serum administration at high dose significantly decreased the level of Bax and increased that of Bcl-xl ($P < 0.01$). YC-1 showed similar inhibitory effect on Dima decoction serum as describe above.

Levels of key genes in HIF-1 α /BNIP3/Beclin-1 signaling pathway

Table 3 presents the mRNA levels of HIF-1 α , BNIP3 and Beclin-1 in HT-29 cells. The mRNA levels of HIF-1 α ,

BNIP3 and Beclin-1 were significantly elevated in contrast to the NC group ($P < 0.01$). Consistent with the previous results of proteins in autophagy signaling pathway, Mesalazine and Dima decoction serum treatment obviously increased the mRNA levels of these genes in contrast to the model group ($P < 0.001$, $P < 0.01$ or $P < 0.05$). The combination treatment of Dima decoction serum with YC-1 notably reduced the mRNA levels of HIF-1 α , BNIP3 and Beclin-1, either falling below or matching those observed in the model group ($P < 0.01$ or $P > 0.05$).

DISCUSSION

Decades ago, reports emerged regarding the utilization of Chinese Medicine for treating inflammatory bowel disease (KANG *et al.*, 2023). Yet, Previous molecular biology studies on using Chinese medicine to treat ulcerative colitis were very limited, it confirms that the therapeutic impact of Dima decoction was assessed using UC model rats, and its underlying molecular mechanisms were explored with HT-29 inflammatory cells. The main clinical manifestations of UC were observed after modeling, such as diarrhea, pus and blood stools, positive occult blood test in stool routine, reduced water and diet, decreased activity, low and yellow urine, sticky and unformed stools (DU *et al.*, 2022). Dima decoction significantly improve the clinical manifestations. In addition, the improvement of colonic histopathology in UC rats further confirmed the therapeutic effect of Dima decoction.

The microstructure changes of colon tissues were observed by TEM, results showed that UC caused mitochondrial damage and autophagosomes loss, as well as destruction of tight junctions, echoing earlier findings (Wang *et al.*, 2021; Zhou *et al.*, 2020). Nevertheless, Dima decoction treatment reversed these alterations, suggesting that its therapeutic efficacy in UC may be linked to the enhancement of autophagy. To validate this hypothesis, YC-1, an autophagy inhibitor, was employed to impede the autophagic process. Results showed that compared with Dima decoction treatment, combination treatment of Dima decoction and YC-1 showed deterioration of autophagy, which was similar to model group in terms of microstructure. Moreover, this deteriorating phenotype was also observed by colonic histopathology. Above results indicating that Dima decoction might relieve UC by stimulating autophagy. Autophagy is essential in the pathogenesis of ulcerative colitis by maintaining Intestinal equilibrium, preserving epithelial barrier cohesion, enhancing antimicrobial defenses, and modulating immune responses in the gut (Zhang *et al.*, 2020). Emerging data indicates that the dysregulation of the autophagy process may disturb the function of intestinal mucosal cells and perturb immune balance in the gut, leading to inappropriate immune responses and subsequent inflammation (Wang *et al.*,

2021). It is also crucial for treating UC to regulate and maintain pro-inflammatory cytokines balance while restoring the body's normal immune function (Kang *et al.*, 2023). Cytokines directly contribute to damage to the mucosal lining and tissues, with some subsequently prompting inflammation specific to the disease in UC (Zhou *et al.*, 2020). For the purpose of this investigation, drug-containing serum was prepared and applied to HT-29 cells to measure the change of inflammatory response. ELISA results showed that serum from model group rats significantly promoted pro-inflammatory mediators production and reduced the levels of anti-inflammatory mediators. It's noteworthy that the administration of Dima decoction serum significantly reversed this alteration, reducing the concentrations of pro-inflammatory mediators and concurrently boosting those of anti-inflammatory mediators. Moreover, to confirm the anti-inflammatory effect of Dima decoction serum was related to autophagy, YC-1 was added to HT-29 cells after Dima decoction serum treatment. Results showed that YC-1 addition obviously inhibited the effect of Dima decoction serum, indicating the crucial function of autophagy.

Mitophagy is closely related to the HIF-1 α /BNIP3/Beclin-1 signaling pathway (Gusev *et al.*, 2021). HIF-1 α is an oxygen-sensitive transcription activator, vital in repairing the cellular oxygen environment during hypoxia. BNIP3, a downstream target gene of HIF-1, directly regulates cell death. Usually, the level of BNIP3 expression is minimal, but increased during hypoxia (Yang *et al.*, 2019). This not only controls cell death but also positively influences the regulation of cell autophagy and mitophagy processes (Yu *et al.*, 2019). Beclin-1 is also crucial in regulating mitophagy, which is achieved by interacting with BNIP3. Under severe conditions, oxidative stress is initiated, leading to a hypoxic state. Moreover, activated HIF-1 α significantly reduces the binding between Beclin-1 and Bcl-2 by upregulating BNIP3 expression. Beclin-1 is liberated from the Bcl-x1/Beclin-1 or Bcl-2/Beclin-1 complex. The unbound Beclin-1 can then interact with various proteins, assembling into a type III phosphatidylinositol-3-kinase complex (PI3K complex). This complex regulates the positioning of downstream autophagy-related Atg proteins within the autophagy precursor structure, thereby initiating mitophagy. Due to the inflammatory activity during the onset of UC, the level of mitochondrial autophagy in intestinal epithelial cells will increase in a reactive manner, promoting cell repair and combating inflammation. The experimental results showed a notable elevation in the levels of HIF-1 α /BNIP3/Beclin-1 in the model group relative to the blank group, confirming this relationship. The levels of HIF-1 α /BNIP3/Beclin-1 expression were significantly higher in each dosage group of Dima decoction compared with those in the model group. This suggests that the application of Dima decoction enhances the activity of mitochondrial autophagy in the intestinal epithelium, aligning with the inflammatory repair status observed in

the HE staining results across all groups. The regulatory impact of HIF-1 α /BNIP3/Beclin-1 in the medium and high dose groups of Dima decoction is notably more pronounced when contrasted with the low dose group, and no significant difference is observed compared to the mesalazine group. These findings suggest that Dima decoction may counteract UC inflammatory activity through the regulation of proteins in the HIF-1 α /BNIP3/Beclin-1 pathway.

Because LC3 is involved in the production of autophagosomes, it is the main protein for detecting autophagy (Ohnstad *et al.*, 2020). The integrity of autophagy flow can be assessed through LC3 detection. The Western blot findings in this study demonstrated that treatment with Dima decoction serum significantly increased the levels of LC3B-II and enhanced the LC3B-II/I ratio compared to the model group. This indicates that Dima decoction might exert a protective effect on intestinal epithelial cells by enhancing autophagy. Moreover, compared to the model group, treatment with Dima decoction serum not only elevated the levels of HIF-1 α , BNIP3, and Beclin-1 proteins but also upregulated the mRNA levels of these genes, aligning with previous speculation. In this study, the levels of the anti-apoptotic protein Bcl-xL were notably reduced in the model group, while those of the pro-apoptotic protein Bax were increased, consistent with a prior study (Wei, Y. *et al.*, 2023). However, this change was reversed after Dima decoction serum treatment, suggesting that both autophagy promoting and apoptosis inhibiting were involved in maintaining colon homeostasis. The way in which Dima decoction influences mitophagy in UC rats aligns with the principles of traditional Chinese medicine, such as "invigorating qi to invigorate the spleen and "promoting blood circulation and detoxification. This offers an objective perspective on the essence of these principles in the context of Chinese medicine, viewed through the lens of contemporary medical practices.

CONCLUSION

Dima decoction showed good therapeutic effect on UC and can significantly reduce the pathological changes colonic tissue in UC rats. In terms of its mechanism, treatment with Dima decoction activated the HIF-1 α /BNIP3/Beclin-1 signaling pathway, consequently promoting mitophagy. In parallel, the excessive inflammatory response was alleviated after Dima decoction serum treatment in HT-29 cells. Moreover, the anti-apoptosis effect of Dima decoction serum was also observed. According to the experimental findings, it can be inferred that Dima decoction possesses the ability to suppress inflammation by enhancing autophagy and inhibiting apoptosis. Consequently, Dima decoction could serve as a standard anti-inflammatory treatment regimen for individuals experiencing mild to moderate active ulcerative colitis. Owing to the multitargeting effect of

Dima decoction and the complexity of UC pathogenesis, the efficacy of Dima decoction may be related to a variety of cellular signaling pathways, which is needed for further research in the future.

ACKNOWLEDGEMENTS

This work was supported by the key Project of Natural Science Research of Universities in Anhui Province, Grant/Award Numbers: 2022AH050490, KJ2020A0445.

REFERENCES

- Agrawal M and Jess T (2022). Implications of the changing epidemiology of inflammatory bowel disease in a changing world. *United European Gastroenterol J.*, **10**(10): 1113-1120.
- Chen S, Yang J, Wang F, Gao X, Liu Q, Liu Q, Zhang Y, and Yu Y (2022). Rapamycin enhanced sensitivity of HT-29 cells to 5-fluororacil by promoting autophagy. *Bull. Exp. Biol. Med.*, **173**(4): 448-453.
- Chen Y, Li J, Li S, Cheng Y, Fu X, Li J and Zhu L (2023). Uncovering the novel role of NR1D1 in regulating bnip3-mediated mitophagy in ulcerative colitis. *Int. J. Mol. Sci.*, **24**(18): 14222.
- Crespo I, San-Miguel B, Prause C, Marroni N, Cuevas MJ, Gonzalez-Gallego J and Tunon MJ (2012). Glutamine treatment attenuates endoplasmic reticulum stress and apoptosis in TNBS-induced colitis. *PLoS One*, **7**(11): e50407.
- Cui L, Guan X, Ding W, Luo Y, Wang W, Bu W, Song J, Tan X, Sun E, Ning Q, Liu G, Jia X and Feng L (2021). *Scutellaria baicalensis* Georgi polysaccharide ameliorates DSS-induced ulcerative colitis by improving intestinal barrier function and modulating gut microbiota. *Int. J. Biol. Macromol.*, **166**: 1035-1045.
- Du N, Liu R, Zhu X and Zhang Z (2022). Efficacy of Sishen Wan on dinitrobenzene sulfonic acid-induced ulcerative colitis and its effect on toll-like receptor 2/interleukin-1 receptor-associated kinase-4/nuclear factor- κ B signal pathway. *J. Tradit. Chin. Med.*, **42**(4): 565-575.
- Du Plessis M, Davis T, Loos B, Pretorius E, de Villiers W JS and Engelbrecht AM (2021). Molecular regulation of autophagy in a pro-inflammatory tumour microenvironment: New insight into the role of serum amyloid A. *Cytokine Growth Factor Rev.*, **59**: 71-83.
- Gao S, Sun D, Wang G, Zhang J, Jiang Y, Li G, Zhang K, Wang L, Huang J and Chen L (2016). Growth inhibitory effect of paratocarpin E, a prenylated chalcone isolated from *Euphorbia humifusa* Wild. by induction of autophagy and apoptosis in human breast cancer cells. *Bioorg. Chem.*, **69**: 121-128.
- Gui G, Meng SS, Li LJ, Liu B, Liang HX and Huangfu CS (2016). Sodium nitrite enhanced the potentials of migration and invasion of human hepatocellular

- carcinoma SMMC-7721 cells through induction of mitophagy. *Acta Pharm. Sin.*, **51**(1): 59-67.
- Gusev E, Solomatina L, Zhuravleva Y and Sarapultsev A (2021). The pathogenesis of end-stage renal disease from the standpoint of the theory of general pathological processes of inflammation. *Int. J. Mol. Sci.*, **22**(21): 11453.
- Hooper KM, Barlow PG, Stevens C and Henderson P (2017). Inflammatory bowel disease drugs: A Focus on Autophagy. *J. Crohns. Colitis*, **11**(1): 118-127.
- Kang H, Wang H, Ji J, Yan L and Zhou Z (2023). Qingchi San treats ulcerative colitis in mice by inhibiting the nuclear factor-kappa B signaling pathway and Nucleotide-binding oligomerization domain, leucine-rich repeat and pyrin domain-containing 3 inflammasome formation. *J. Tradit. Chin. Med.*, **43**(1): 68-77.
- Karsli-Uzunbas G, Guo JY, Price S, Teng X, Laddha SV, Khor S, Kalaany NY, Jacks T, Chan CS, Rabinowitz JD and White E (2014). Autophagy is required for glucose homeostasis and lung tumor maintenance. *Cancer Discov.*, **4**(8): 914-927.
- Larabi A, Barnich N and Nguyen HTT (2020). New insights into the interplay between autophagy, gut microbiota and inflammatory responses in IBD. *Autophagy*, **16**(1): 38-51.
- Lemasters JJ (2005). Selective mitochondrial autophagy, or mitophagy, as a targeted defense against oxidative stress, mitochondrial dysfunction and aging. *Rejuvenation Res.*, **8**(1): 3-5.
- Ng SC, Shi HY, Hamidi N, Underwood FE, Tang W, Benchimol EI, Panaccione R, Ghosh S, Wu JCY, Chan FKL, Sung JY and Kaplan GG (2017). Worldwide incidence and prevalence of inflammatory bowel disease in the 21st century: A systematic review of population-based studies. *The Lancet*, **390**(10114): 2769-2778.
- Niu W, Chen X, Xu R, Dong H, Yang F, Wang Y, Zhang Z and Ju J (2021). Polysaccharides from natural resources exhibit great potential in the treatment of ulcerative colitis: A review. *Carbohydr. Polym.*, **254**: 117189.
- Ohnstad A, Delgado J, North B, Nasa I, Kettenbach A, Schultz S and Shoemaker C (2020). Receptor mediated clustering of FIP200 bypasses the role of LC3 lipidation in autophagy. *EMBO J.*, **39**(24): e104948.
- Tan Y, Yin L, Sun Z, Shao S, Chen W, Man X, Du Y and Chen Y (2020). Astragalus polysaccharide exerts anti-Parkinson via activating the PI3K/AKT/mTOR pathway to increase cellular autophagy level *in vitro*. *Int. J. Biol. Macromol.*, **153**: 349-356.
- Vardareli E, Dundar E, Angin K, Saricam T and Inal M (2003). Effects of intrarectal and intraperitoneal N(G)-nitro-L-arginine methyl ester treatment in 2,4,6-Trinitrobenzenesulfonic acid induced colitis in rats. *Exp. Toxicol. Pathol.*, **55**(4): 271-276.
- Wang B, Gong Z, Zhan J, Yang L, Zhou Q and Yuan X (2021). Xianglian pill suppresses inflammation and protects intestinal epithelial barrier by promoting autophagy in DSS induced ulcerative colitis mice. *Front. Pharmacol.*, **11**: 594847.
- Watanabe S, Fukushi S, Harada T, Shimojima M, Yoshikawa T, Kurosu T, Kaku Y, Morikawa S and Saijo M (2020). Effective inactivation of Nipah virus in serum samples for safe processing in low-containment laboratories. *Virology*, **17**(1): 151.
- Wei Y, Zhang L, Wang C, Li Z, Luo M, Xie G, Yang X, Li M, Ren S, Zhao D, Gao R and Gong JN (2023). Anti-apoptotic protein BCL-XL as a therapeutic vulnerability in gastric cancer. *Anim. Model Exp. Med.*, **6**(3): 245-254.
- Xu C, Wang P, Lin C, Luo Z, Huang Y, Zhao Z and Yang C (2018). The protective and therapeutic effects of total flavonoids of Astragalus against bleomycin-induced pulmonary fibrosis are through the enhancement of autophagy. *J. Tradit. Chin. Med. Sci.*, **5**(4): 380-389.
- Yang L, Wu J, Xie P, Yu J, Li X, Wang J and Zheng H (2019). Sevoflurane postconditioning alleviates hypoxia-reoxygenation injury of cardiomyocytes by promoting mitochondrial autophagy through the HIF-1/BNIP3 signaling pathway. *Peer J.*, **7**: e7165.
- Yu H, Chen B and Ren Q (2019). Baicalin relieves hypoxia-aroused H9c2 cell apoptosis by activating Nrf2/HO-1-mediated HIF1 α /BNIP3 pathway. *Artif. Cell. Nanomed. B.*, **47**(1): 3657-3663.
- Zhang S, Li Z, Wang D, Xu T, Fan M, Cheng M and Miao C (2020). Aggravated ulcerative colitis caused by intestinal Metrn1 deficiency is associated with reduced autophagy in epithelial cells. *Acta. Pharmacol. Sin.*, **41**(6): 763-770.
- Zhang SM, Fan B, Li YL, Zuo ZY and Li GY (2023). Oxidative stress-involved mitophagy of retinal pigment epithelium and retinal degenerative diseases. *Cell. Mol. Neurobiol.*, **43**(7): 3265-3276.
- Zhang Z, Qiao D, Zhang Y, Chen Q, Chen Y, Tang Y, Que R, Chen Y, Zheng L, Dai Y and Tang Z (2022). *Portulaca oleracea* L. extract ameliorates intestinal inflammation by regulating endoplasmic reticulum stress and autophagy. *Mol. Nutr. Food Res.*, **66**(5): 2100791.
- Zhong Y, Xiao Q, Kang Z, Huang J, Ge W, Wan Q, Wang H, Zhou W, Zhao H and Liu D (2022). Astragalus polysaccharide alleviates ulcerative colitis by regulating the balance of Tfh/Treg cells. *Int. Immunopharmacol.*, **111**: 109108.
- Zhou C, Li L, Li T, Sun L, Yin J, Guan H, Wang L, Zhu H, Xu P, Fan X, Sheng B, Xiao W, Qiu Y and Yang H (2020). SCFAs induce autophagy in intestinal epithelial cells and relieve colitis by stabilizing HIF-1 α . *J. Mol. Med.*, **98**(8): 1189-1202.
- Zhou X, Yang J, Qu X, Meng J, Miao R and Cui S (2020). M10, a myricetin-3-O-b-D-lactose sodium salt, prevents ulcerative colitis through inhibiting necroptosis in mice. *Front. Pharmacol.*, **11**: 557312.